Science Advances
AAAS

advances.sciencemag.org/cgi/content/full/4/8/eaat2142/DC1

Supplementary Materials for

DNA methylation regulates transcriptional homeostasis of algal endosymbiosis in the coral model Aiptasia

Yong Li, Yi Jin Liew, Guoxin Cui, Maha J. Cziesielski, Noura Zahran, Craig T. Michell, Christian R. Voolstra, Manuel Aranda*

*Corresponding author. Email: manuel.aranda@kaust.edu.sa

Published 15 August 2018, *Sci. Adv.* **4**, eaat2142 (2018)
DOI: 10.1126/sciadv.aat2142

The PDF file includes:

Fig. S1. Circos visualization of different data at the genome-wide level.
Fig. S2. Methylated genes in Aiptasia have lower CpG O/E.
Fig. S3. Methylation patterns.
Fig. S4. Sequence conservation of histone H3 homologs.
Fig. S5. Western blot.
Fig. S6. Correlation matrices of replicates.
Fig. S7. Validation of methylation level.
Fig. S8. qPCR validation of gene expression levels.
Fig. S9. Correlation between DNA methylation changes and gene expression changes.

Other Supplementary Material for this manuscript includes the following:

(available at advances.sciencemag.org/cgi/content/full/4/8/eaat2142/DC1)

Table S1 (Microsoft Excel format). Aiptasia DMGs.
Table S2 (Microsoft Excel format). Aiptasia DEGs.
Table S3 (Microsoft Excel format). GO enrichment analysis of DMGs—biological process.
Table S4 (Microsoft Excel format). GO enrichment analysis of DMGs—molecular function.
Table S5 (Microsoft Excel format). GO enrichment analysis of DMGs—cellular component.
Table S6 (Microsoft Excel format). GO enrichment analysis of DEGs—biological process.
Table S7 (Microsoft Excel format). GO enrichment analysis of DEGs—molecular function.
Table S8 (Microsoft Excel format). GO enrichment analysis of DEGs—cellular component.
Table S9 (Microsoft Excel format). KEGG pathway enrichment analysis of DEGs.
Table S10 (Microsoft Excel format). KEGG pathway enrichment analysis of DMGs.
Table S11 (Microsoft Excel format). KEGG pathway enrichment analysis of DEMGs and statistics of symbiosis related pathways' ranks.
Table S12 (Microsoft Excel format). Cnidarian-dinoflagellate symbiosis–related Aiptasia genes.

Table S13 (Microsoft Excel format). qPCR primers for gene expression validation.
Table S14 (Microsoft Excel format). qPCR raw C_t (cycle threshold) values for gene expression validation.
Table S15 (Microsoft Excel format). qPCR: $\Delta\Delta C_t$ approach for fold-change calculations.
Table S16 (Microsoft Excel format). Primers for bisulfite PCR-based methylation validation.

Supplementary Figures

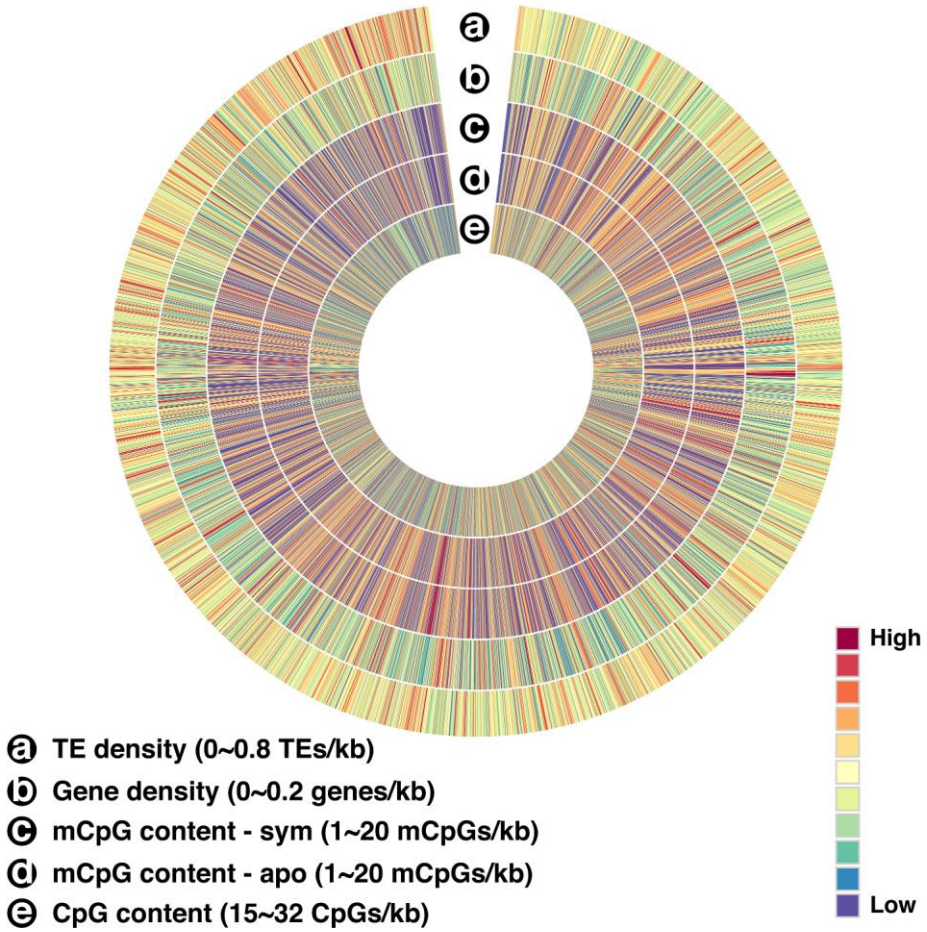

Fig. S1. Circos visualization of different data at the genome-wide level. (**a**) TE density. (**b**) Gene density. (**c**) Fraction of methylated CpGs in symbiotic samples. (**d**) Fraction of methylated CpGs in aposymbiotic samples. (**e**) CpG content.

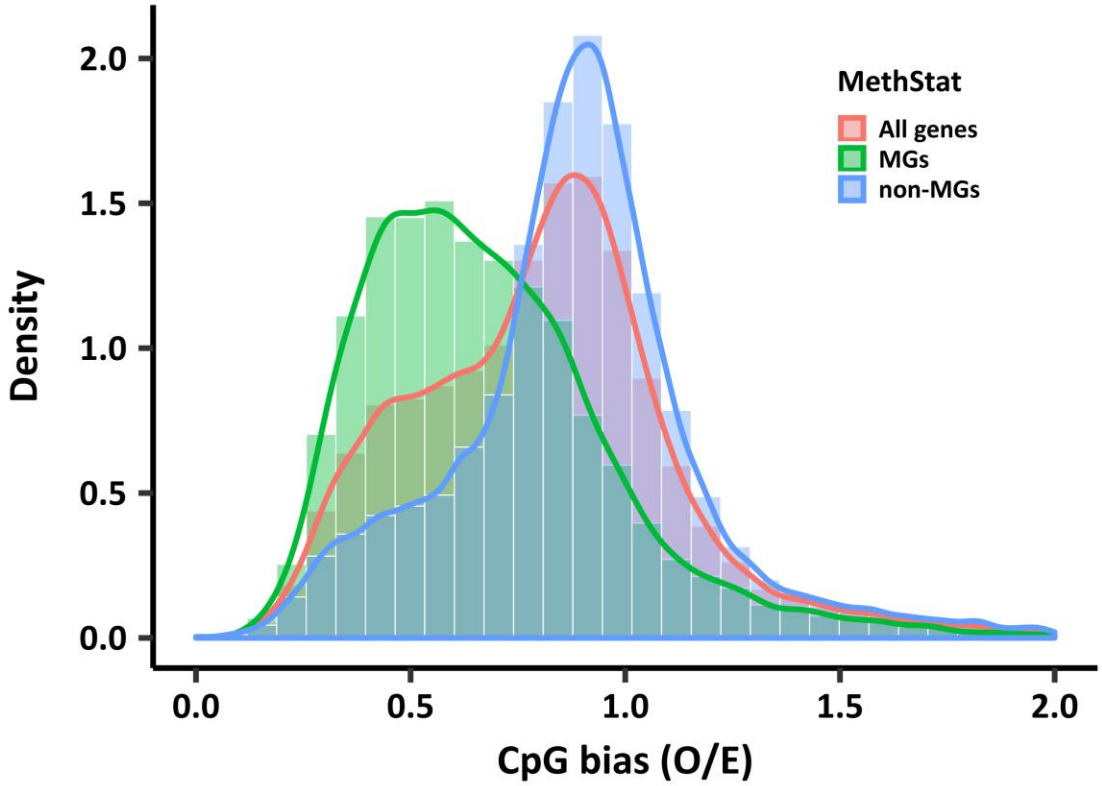

Fig. S2. Methylated genes in Aiptasia have lower CpG O/E. CpG distribution of methylated genes (represented by red curve) peaks at around 0.5, which is lower than in unmethylated genes (represented by green curve) peaking at around 0.9. mC to T conversion skews the CpG O/E distribution of all genes as expected (represented by blue curve), but methylated and unmethylated genes still show a large overlap of their CpG O/E distributions. These results indicate that gene body methylation cannot be accurately inferred from CpG O/E in Aiptasia.

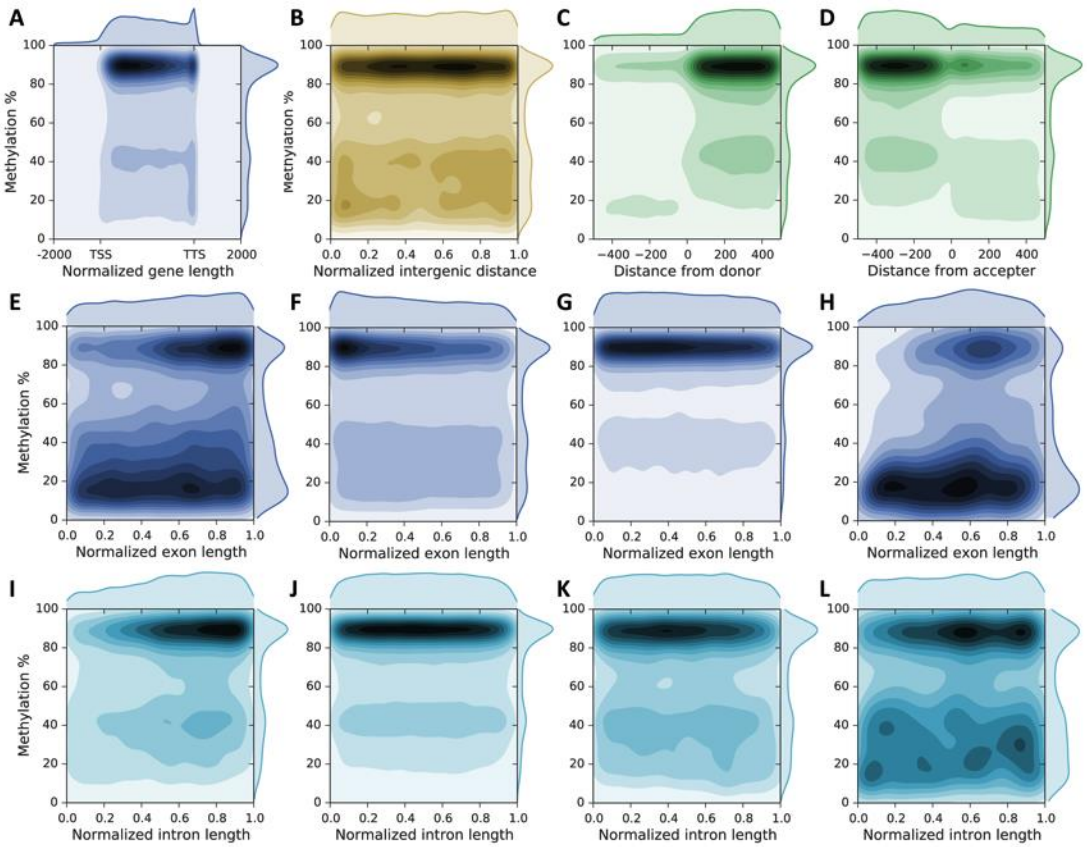

Fig. S3. Methylation patterns. (**A**) DNA methylation is mainly located in the proximal part of gene bodies with slightly decreasing levels towards the end. (**B**) Methylation pattern over intergenic regions. (**C**) Methylation pattern around splice donor sites show increasing levels immediately after donor sites. (**D**) Methylation pattern around acceptor sites show decreasing levels immediately after splice acceptor sites. (**E**) Methylation pattern over initial exons show increasing methylation levels (3,147 exons with 35,885 methylation sites were used). (**F**) Methylation pattern over internal exons shows decreasing methylation levels (7,977 exons with 139,009 methylation sites were used). (**G**) Methylation pattern over terminal exons shows decreasing methylation levels (7,905 exons with 102,162 methylation sites were used). (**H**) Methylation pattern over introns from single-exon genes follows a similar trend as observed for

multi exon genes with increasing methylation levels in the proximal and decreasing levels in the posterior part of the exon (298 exons with 4,735 methylation sites were used). (**I**) Methylation pattern over initial introns shows increasing methylation levels (3,381 introns with 39,262 methylation sites were used). (**J**) Methylation pattern over internal introns maintains stable methylation levels (7,371 introns with 211,950 methylation sites were used). (**K**) Methylation levels over terminal introns decrease slightly (3,959 introns with 34,246 methylation sites were used). (**L**) Methylation levels over introns from one-intron genes change gently with initial increase followed by a decrease (1,055 introns with 10,709 methylation sites).

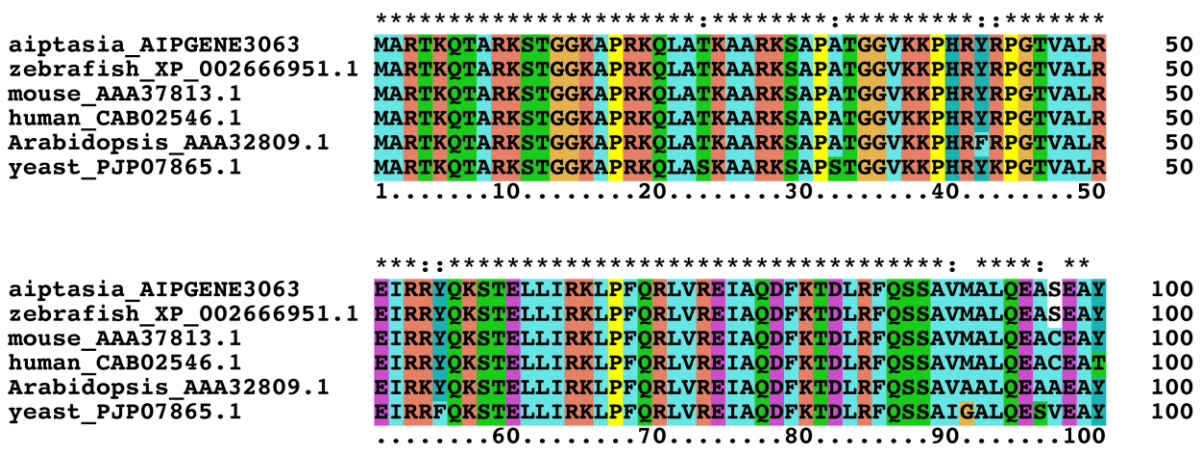

Fig. S4. Sequence conservation of histone H3 homologs. Sequence conservation of Aiptasia histone H3 protein and histone H3 homologs from species for which antibody (ab9050, Abcam) has previously been validated. The N-terminal tail of Aiptasia H3 is identical to the fragment from the zebrafish *Danio rerio* (the first 100 amino acid fragment from human was used to produce this antibody).

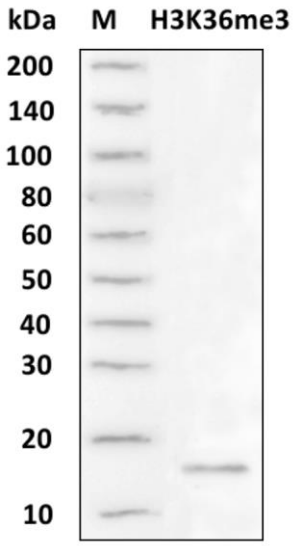

Fig. S5. Western blot. Western blot result for antibody affinity validation, target band is 15kDa in size as expected from molecular weight analysis.

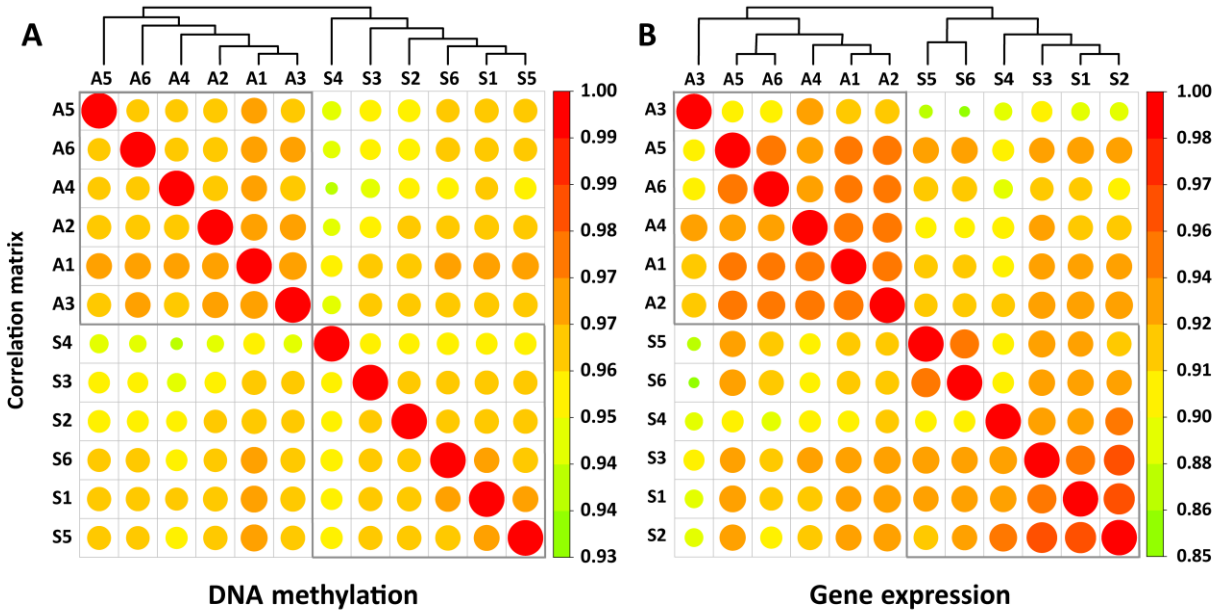

Fig. S6. Correlation matrices of replicates. Correlation matrices of replicates based on median DNA methylation level of genes (**A**) and log gene expression values (base 2) (**B**). Replicates from the same symbiotic states showed higher correlation and clustered together both based on DNA methylation as well as gene expression profiles, further supporting the findings obtained from the PCA analyses (figure 4) that changes in DNA methylation and expression are symbiotic state specific.

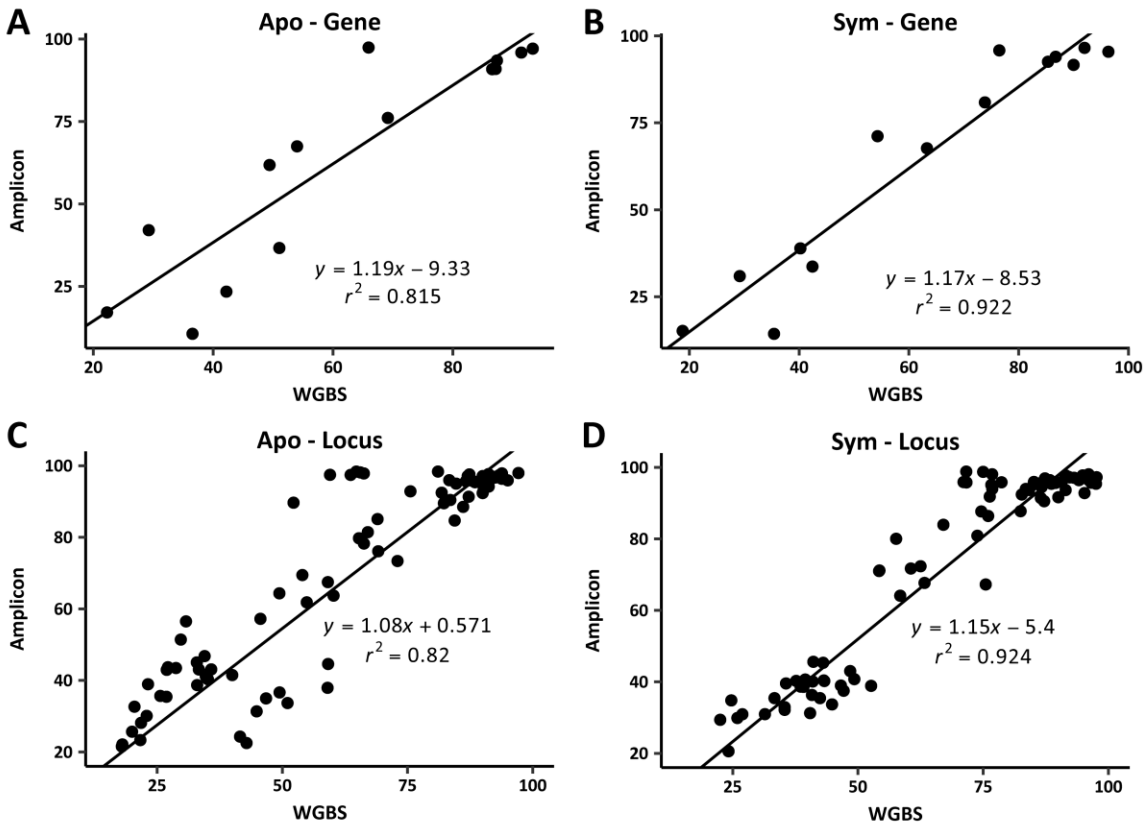

Fig. S7. Validation of methylation level. Validation of methylation level using bisulfite PCR on selected genes. (**A** and **B**) validation of methylation level on genes (median methylation levels of methylated CpGs were used to represent genes). (**C** and **D**) validation of methylation level on locus (methylated CpGs). WGBS: whole genome bisulfite sequencing; Amplicon: MiSeq sequencing results of bisulfite PCR amplicons on selected genes.

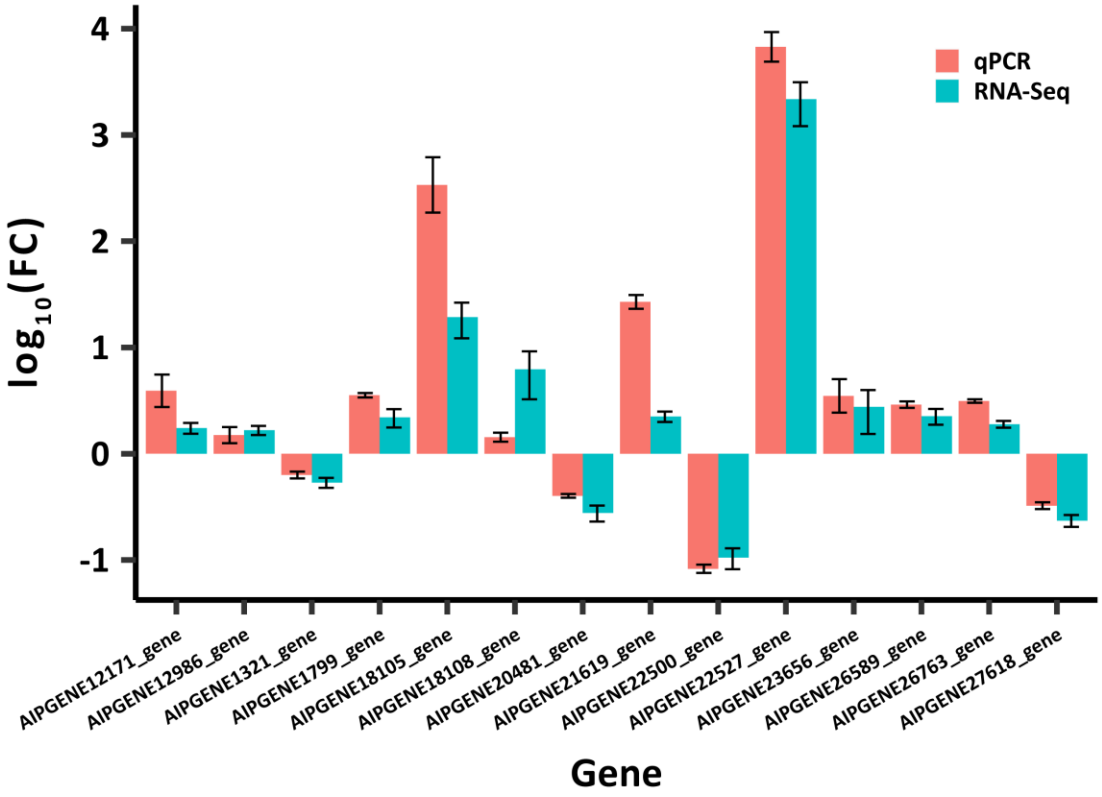

Fig. S8. qPCR validation of gene expression levels. Validation of gene expression changes using qPCR. Expression levels are shown as $\log_{10}$(fold change). All genes show similar expression changes as determined by RNA-Seq and qPCR.

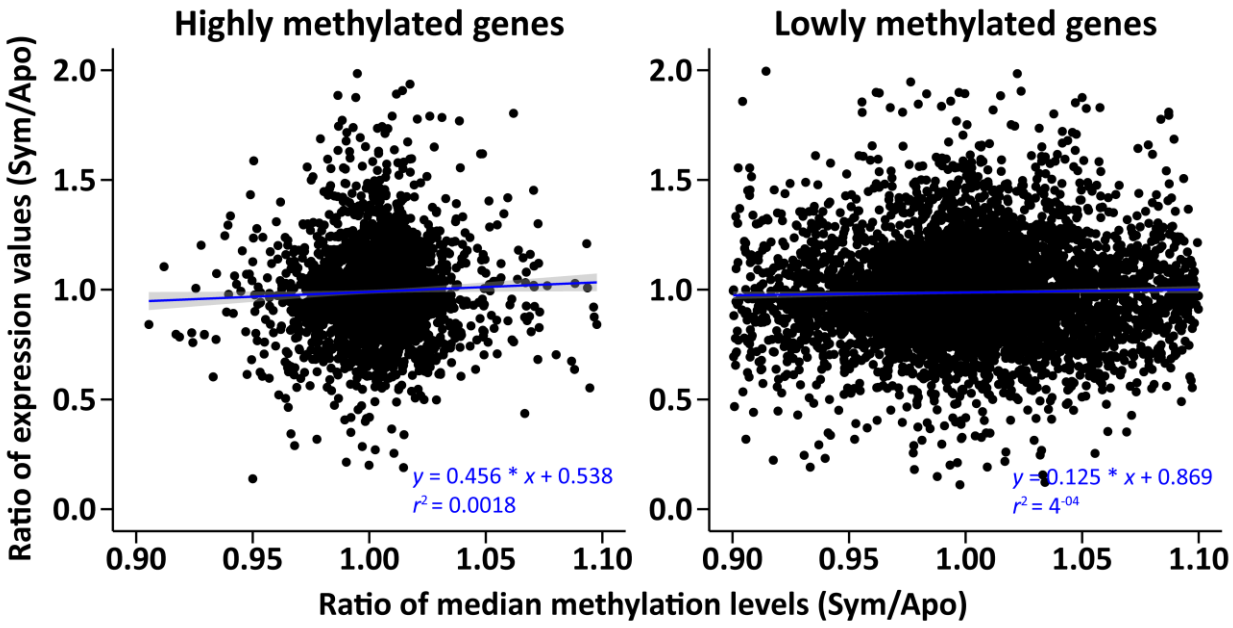

Fig. S9. Correlation between DNA methylation changes and gene expression changes. DNA methylation changes and gene expression changes have very weak correlation. Highly methylated genes: the methylated genes have median methylation level ≥70%; lowly methylated genes: other methylated genes.